Composites: Part B 60 (2014) 341–349

Contents lists available at ScienceDirect

Composites: Part B

journal homepage: www.elsevier.com/locate/compositesb

The synthesis of a novel graphene-based inorganic–organic hybrid flame retardant and its application in epoxy resin

Zehao Wang [a], Ping Wei [a,*], Yong Qian [a], Jiping Liu [b]

[a] School of Chemistry and Chemical Engineering, Shanghai Jiao Tong University, 800 Dongchuan Road, Shanghai 200240, PR China
[b] National Laboratory of Flame Retardant Materials, School of Materials Science and Engineering, Beijing Institute of Technology, Beijing 100081, PR China

ARTICLE INFO

Article history:
Received 21 January 2013
Received in revised form 9 November 2013
Accepted 22 December 2013
Available online 2 January 2014

Keywords:
A. Polymer–matrix composites (PMCs)
A. Hybrid
D. Thermal analysis
E. Thermosetting resin

ABSTRACT

In this paper, a novel graphene-based inorganic–organic hybrid flame retardant (GFR) was prepared via sol–gel reaction of FGO and phenyl-bis-(triethoxysilylpropyl) phosphamide (PBTP) and characterized by FT-IR, XPS, XRD, TGA and AFM. The influence of the GFR on the thermal stability and flame retardance of epoxy resin composites were characterized by TGA, LOI as well as micro-cone, which indicated that GFR brought a good effect in enhancing the residual char and flame retardance of epoxy composites. The dynamic mechanical properties and electrical properties of EP composites were also analyzed.

1. Introduction

Epoxy resin is widely used in electrical engineering components because of its superior mechanical and chemical properties including high hardness, excellent electrical strength and chemical resistance, etc. [1]. However, poor fire resistance is still a challenging problem that limits its extensive applications especially in semiconductor encapsulation and printed circuit board industries [2,3]. Halogen free flame retardants with their environment friendly property has become a new trend of replacing the original position of halogen-containing flame retardants in improving fire resistance of epoxy resin [4,5]. Phosphorus, nitrogen and silicon are all environment friendly flame-retarding elements. Phosphorus containing flame retardants act both in the vapor phase and the condensed phase, not only can capture free radical to suppress combustion but also promote char formation on polymer surface [6]. Nitrogen can play as foaming agent, being synergetic with phosphorus to form effective intumescent flame-retarding system [7]. Silicon with superior thermal and thermo-oxidative stability can convert to stable silicon dioxide under pyrolysis thus improve the char barrier to inhibit flammable products from diffusing to the flame and to insulate the polymer surface from heat and air [8,9]. The synergistic effect of Si, P and N elements in epoxy resins also prove the better performance of thermal stability [10,11].

As reported, graphene exhibits remarkable values of fracture strength, Young's modulus, specific surface, electron mobility and thermal conductivity, etc. [12], which make graphene derivatives span a variety of application such as sensors, batteries, hydrogen storage, electronic devices and nanofillers used to enhance the application performance of polymers [13]. However, due to the high surface area and strong vander Waals force, the re-aggregating phenomenon is inclined to appear between graphene sheets, which limit its' use in polymer matrix [14]. The problem is usually solved by covalent functionalization. After oxidation, rich oxygen-containing groups (e.g., hydroxyl, epoxide, carboxyl and carbonyl groups, etc.) are brought to the surface of graphene sheets [15]. Through further chemically functionalizing the graphene oxide (GO), grafting the organic molecules on GO was widely adopted in improving GO's dispersion and its thermal stability [16,20].

Graphene with high thermal resistance may act as a barrier in polymer during combustion [17] which can slow down the heat release and block combustible fragments into flame area [12,18]. Actually, incorporating graphene alone as nanofiller alone into epoxy matrix failed to exhibited excellent flame retardance [2], hybrid materials combining the properties of graphene and flame retardant elements has aroused new interests [19,21]. Guo et al. [3]. prepared FGO grafted with phosphorus-containing molecule and prepared FGO/EP composites, of which the total heat released (THR) lower than that of GO/EP composites but no obvious differences were seen for the char residual formation between two composites.

In this work, a novel graphene-based inorganic–organic hybrid flame retardant (GFR) was prepared via sol–gel reaction of FGO and phenyl-bis-(triethoxysilylpropyl) phosphamide (PBTP). First, we used benzene phosphorous oxydichloride and 3-aminopropyltri-

* Corresponding author. Tel.: +86 21 34202509; fax: +86 21 54741297.
E-mail address: pingwei@sjtu.edu.cn (P. Wei).

1359-8368/$ - see front matter © 2013 Elsevier Ltd. All rights reserved.
http://dx.doi.org/10.1016/j.compositesb.2013.12.033

ethoxysilane to synthesize phenyl-bis-(triethoxysilylpropyl) phosphamide (PBTP). Second, chemically functionalized GO sheets were obtained through the reaction between the trialkoxy groups on PBTP and the hydroxyl groups on the GO surface. Finally, GFR was obtained by embedding GO sheets into PBTP bulk monoliths via sol–gel method. The novel flame retardant combines flame retardant elements phosphorus nitrogen and silicon together, with which the epoxy resin incorporated not only remarkably enhanced the amount of char residual and flame retardance but also obtained higher storage modulus at low loading of GFR. In addition, the dielectric property and electric conductivity of epoxy resin was not affected by the addition of graphene, maintaining its application in electric insulation industry.

2. Experimental

2.1. Materials

3-Aminopropyltriethoxysilane was provided by Shanghai Rising Chemical Co., Ltd. Benzene phosphorous oxydichloride was purchased from Jiangsu Changyu Chemical Co., Ltd. Epoxy resin, D.E.R. 331 was supplied by the Dow Chemical. Epoxy equivalent weight (EEW) of D.E.R. 331 was 188. Polyamide 650 was provided by Zhejiang Jinhong Chemical Co., Ltd. Graphite powder (200 mesh) with a purity of >99% was supplied was purchased from Shijiazhuang Kepeng Co., Ltd. Other reagents were purchased from Sinopharm Chemical Reagent Co., Ltd.

2.2. Synthesis of phenyl-bis-(triethoxysilylpropyl) phosphamide (PBTP)

A 0.1 mol 3-aminopropyltriethoxysilane and 0.1 mol triethylamine were dissolved in 80 ml diethyl ether. The mixture solution was then transferred into a three-necked bottle equipped with a reflux condensing tube and mechanical agitator which had been aerated with N_2 for 0.5 h.0.05 mol phenylphosphonic dichloride dissolved in 20 ml diethyl ether, under an ice bath condition, was dropped into the three-necked bottle within 1 h which was controlled by a constant pressure funnel. After addition of phosphorus oxychloride, the mixture was kept stirring for 1 h at 0 °C then raised to 40 °C for 3 h. After reaction, triethylamine hydrochloride was removed through filtration, shortly after which, the filtrate was put to a round flask to remove residual diethyl ether by rotary evaporator. Phenyl-bis-(triethoxysilylpropyl) phosphamide was obtained as light yellow viscous liquid.

2.3. Synthesis of functionalized graphene oxide

To synthesize FGO, at first GO was produced according to a modified Hummers method as reported [22], then 0.1 g GO and 0.3 g PBTP were added to a three-neck flask with 200 ml ethanol and were dispersed by ultrasonication for 60 min, and the homogeneous mixture was stirred for 24 h at 65 °C for silylation. After the reaction finished, the homogeneous PBTP functionalized graphene oxide (FGO) were obtained by centrifugation and washed with absolute ethanol consecutively, then dried in a vacuum.

2.4. Synthesis of graphene flame retardant (GFR)

A 3.0 g ammonia water was dissolved in 50 ml H_2O at room temperature. 0.1 g FGO was well dispersed in 50 ml ethanol in a flask through ultrasonication for 20 min, followed by addition of 0.3 g PBTP, then added into the alkaline solution for expanding the silica netted structure by hydrolysis. After stirring for 2 h, the product was cast into a plastic cylindrical mold to gel at room temperature for 12 h for further hydrolysis then aged at 70 °C for 3 days [22]. The resulting GFR was obtained as powder after the solvent evaporated in a baking oven. The preparation routes of PBTP, FGO and GFR are shown in Scheme 1.

2.5. Preparation of epoxy resin/GFR nanocomposites

A certain amount of GFR is firstly dispersed in THF by ultrasonication and then added into epoxy resin (DER331), the mixture was mechanically stirred at 50 °C for 0.5 h followed by being put into a vacuum oven at 50 °C for 24 h to eliminate the solvent. Polyamide 650# was heated to 50 °C and added into EP/GFR mixture followed by intensive stirring for 20 min. Finally, the mixture was put into a vacuum oven for 10 min to remove air bubble and poured into a polytetrafluoroethylene mold, curing under room temperature for 12 h then at 60 °C for another 4 h, the EP/GFR composite was obtained. EP/GO composite was prepared in the same way.

2.6. Characterization

FT-IR spectroscopy was recorded with PerkinElmer Paragon 1000 instrument. NMR was performed with MERCURYplus 400 (400-MHz) NMR spectrometer with dimethyl sulphoxide-d as solvent. LOI was measured on sheets 100 × 6.5 × 3 mm^3 according to the standard oxygen index test ASTM D 2863-77. Thermogravimetric analysis (TGA) was conducted in nitrogen at a heating rate of 10 °C/min using TA Q5000IR thermogravimetric analyzer. In each case, 10 mg sample was examined under a nitrogen flow rate of 20 ml/min from 50 °C to 800 °C. Scanning electron microscope (SEM) micrographs were obtained by S-2150 (Hitachi Corp., Japan). All the samples were coated with a conductive gold layer. Dynamic Mechanic Analysis (DMA) was performed on a DMA Q800, operating in the Single Cantilever mode at an oscillation frequency of 1 Hz. Data were collected from room temperature to 210 °C at a scanning rate of 3 °C/min. The sample specimens were cut into rectangular bars measuring 1.25 mm × 7.9 mm × 17.5 mm by a diamond saw. The micro-cone calorimeter tests were carried out on pyrolysis-combustion flow calorimeter (PCFC, Govmark, Farmingdale, New York, Model MCC-1). The samples were tested according to ASTM D7309-07. Conductivity of EP/GFR composites were tested on SourceMeter KEITHLEY2400. Dielectric constant is measured by Impedance Analyzer (Aglient 4294A), 100 Hz to 10 MHz, the samples were prepared into diameter = 15 mm, height = 1 mm wafers and coated with a conductive gold layer.

3. Results and discussion

3.1. Characterization of PBTP

Fig. 1 shows the ^1H NMR and ^{31}P NMR spectra of PBTP. The absorption peaks located at 7.46 ppm and 7.85 ppm are attributed to ^1H signal of phenyl group in the PBTP [23]. Other ^1H signals observed at 3.77 ppm, 2.94 ppm, 1.47 ppm, 1.19 ppm, 0.85 ppm and 0.57 ppm are assigned to Si—O—CH_2, N—CH_2—C, C—CH_2—C, O—C—CH_3, P—NH—C and C—CH_2—Si respectively [24]. At the same time, the chemical shift observed at 21.74 ppm is attributed to the unique ^{31}P signal of PBTP. All the above proved the success of synthesis of PBTP.

3.2. Characterization of GO, FGO and GFR

The FT-IR spectra of the GO, FGO, GFR are shown in Fig. 2. In FGO spectra, the new peaks emerged at 1260 cm^{-1} and 920 cm^{-1} [2], comparing with the spectra of GO, correspond to the stretching vibration of P═O and P-N of PBTP respectively. In addition, the appearance of Si—O—C stretching vibration peak at 698 cm^{-1} and

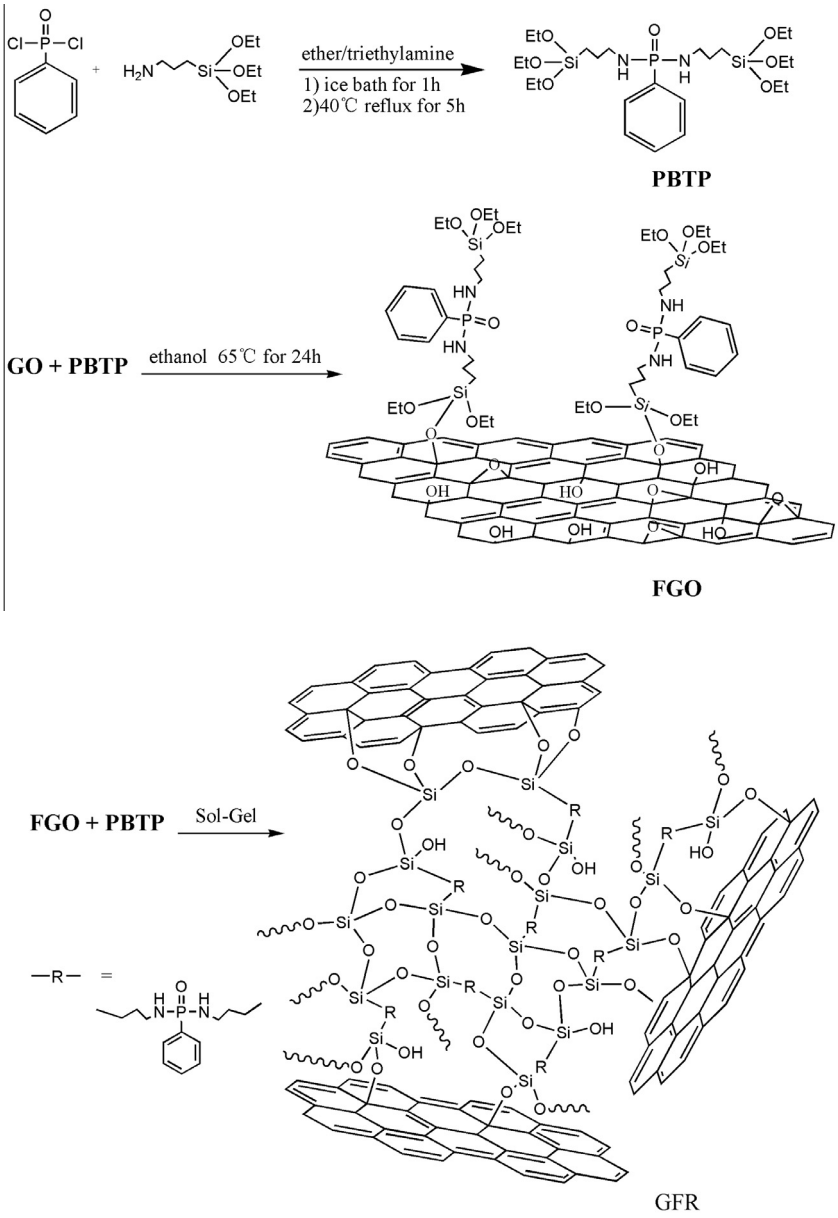

Scheme 1. Preparation route of PBTP, Functionalized GO and GFR.

the disappearance of aromatic-OH peak provided evidence that —OH groups were consumed and converted to Si—O—C by grafting PBTP onto GO sheets [16]. The little peak at 1049 cm^{-1} [22] is due to Si—O—Si groups, resulting from the inevitable partial hydrolysis of the silane group during the silylation process. These newly formed chemical functionalized groups were further verified by X-ray photoelectron spectroscopy (XPS).

Fig. 3 shows the XPS spectra of GO, FGO and GFR. The C1s spectra of GO, FGO are showed in Fig. 3A and B respectively, the Si2p spectra and P2p spectra of FGO are also showed in Fig. 3D and F respectively. In the spectra of GO, the peak at 284.6 eV is attributed to sp^2 carbon of graphite, and the peaks at 285.6 eV, 286.85 eV and 288.5 eV are typically attributed to oxygen containing groups such as hydroxyl, epoxide, and carboxyl [25]. The peaks at 281 eV, 282.95 eV, 285.9 eV in Fig. 3.B are attributed to C—P bond, C—Si bond and C—N bond respectively [26], at the same time, P—N bond (133.3 eV) and C—P=O bond (132.3 eV) [27,28] present in FGO (Fig. 3F), further indentify the presence of PBTP grafting on the graphene surface. Moreover, it is worth noting that the peak of C—OH disappears in the C1s spectra of FGO comparing to which of GO and the strong Si—O—C peak (102.5 eV) [24] appears in Si2p spectra of FGO, which indicate the success of chemical functionalization by the reaction between trialkoxy groups of silane in PBTP and the hydroxyl groups on the GO surface.

The structure of GO, FGO and GFR was evaluated by XRD and the results are shown in Fig. 4. As reported, the typical interlayer spacing of pristine graphite powder is 0.34 nm, however, the (002) peak at 12.4° of GO corresponds to an interlayer distance of 0.71 nm. The increase of the interlayer distance of GO is due to the successful oxide process that brought oxygen-containing group onto GO sheets. After chemical modification, in the spectra of FGO, there is no obvious diffraction peaks of GO observed anymore, which demonstrate the exfoliated and disordered structure formed during sonication and chemical reaction process [29,30]. However, a broad peak appearing at 24.6° indicates a little amount of reclustering.

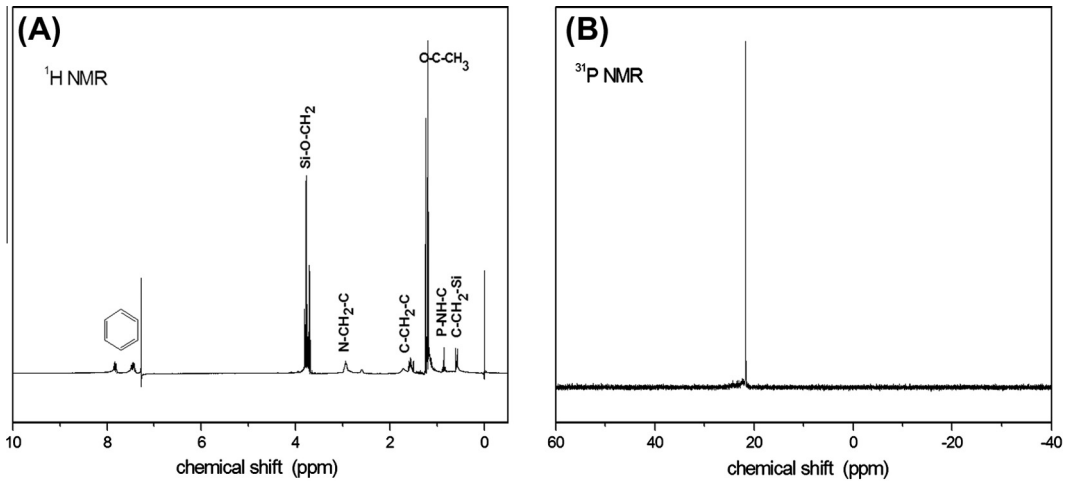

Fig. 1. ^{1}H NMR and ^{31}P NMR of PBTP.

GO and FGO sheets were also imaged by AFM and showed in Fig. 5. The average height of GO sheet is 0.94 nm, after grafting PBTP, the height increase to 1.59 nm. The thicker sheets [31] is possibly due to the PBTP chain grafted on GO surface which indicate that the FGO is successfully obtained in our work.

As to GFR, in FT-IR spectra showed in Fig. 2, all the peaks appear n in the spectra of GFR are similar to those in FGO spectra. Nevertheless, the peak intensity of Si—O—Si groups (1095 cm^{-1}) and of —CH2— groups (2925 cm^{-1} and 2851 cm^{-1}) is much stronger than which in FGO spectra, which confirm the cross-linked netted structure formed by sol–gel process of PBTP and FGO. The C1s and Si2p XPS spectra of GFR are showed in Fig. 3 respectively. Comparing the C1s spectra of GFR to that of FGO, the peak intensity of C—P bond C—Si bond as well as C—N bond of GFR is much stronger than that of FGO, besides, a strong peak of Si—O—Si bond (103.3 eV) in Si2p spectra of GFR that is not obvious in FGO is detected, which is due to the successful formation of the saline structure through the sol–gel process of PBTP and FGO. A new broad peak centred at $2\theta = 21.7°$ is observed in the XRD patterns of GFR (Fig. 4). This peak is typically assigned to coherent diffraction domains of Si—O based backbones [24], which provides another evidence that a graphene-embedded silane netted structure is actually formed.

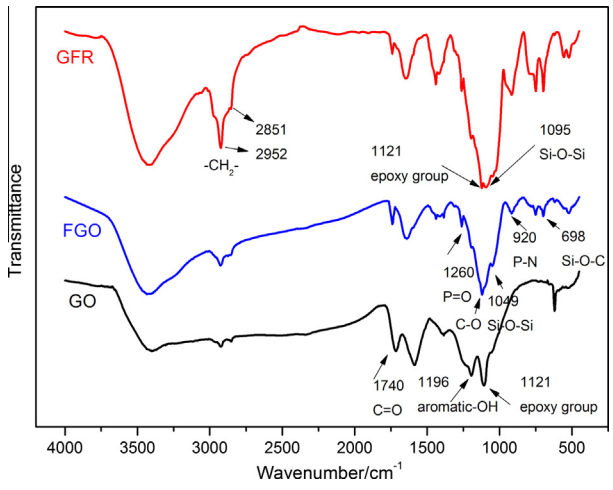

Fig. 2. FT-IR spectra of GO, FGO and GFR.

3.3. Thermal performance

Thermogravimetric analysis of GO, and GFR were carried out in N_2 atmosphere and the results were showed in Fig. 6. Related data are listed in Table 1. There are three mass loss stages in GO. The first stage occurred bellowed 100 °C is due to the evaporation of adsorbed water. The main mass loss is caused by the decomposition of the oxygen-containing groups (hydroxyl, epoxide, carboxyl, etc.) attached to GO, which occurred between 150 °C and 210 °C. The third drop started at 300 °C is attributed to the decomposition of the carbon skeleton of GO, 45.2 wt% of char yield is observed at 800 °C. In the case of FGO and GFR, the onset degradation temperature (at weight loss 5 wt%, $T_{5\%}$) increased from 143 °C to 157 °C and 175 °C respectively, compared with GO, and the weight loss below 210 °C are reduced obviously, indicating that the oxygen-containing group (hydroxyl group) of GO has been replaced by PBTP. Weight loss process from 300 °C to 800 °C are similar to GO, containing the pyrolysis of the carbon structure and the PBTP on GO. The char yield obtained at 800 °C reach 61% and 70% respectively. The increase of $T_{5\%}$ and char yield indicate that the grafted PBTB with rich flame retardant elements (nitrogen, phosphorus, silicon-containing group) can effectively enhance the thermal stability of GO.

3.4. Thermal performance of EP/GFR composites

The TGA and DTG curves of EP and EP/GFR composites in N_2 atmosphere are shown in Figs. 7 and 8. Related data are listed in Table 1. The onset degradation temperatures of EP is 315 °C, compared to which, both of the $T_{5\%}$ of EP/GO and EP/GFR are decreased due to the pyrolysis of the oxygen-containing and PBTP-containing groups on GO respectively. $T_{5\%}$ of EP/GFR is higher than EP/GO, which is caused by the higher thermal stability of GFR than GO according to the discussion before. The temperature of the maximum weight loss rate (T_{max}) is obtained from the DTG curves. T_{max} of the EP/GO composites is quite similar to EP, however, T_{max} of EP/GFR composites decreased by 19–37 °C compared to EP. The decreased $T_{5\%}$ and T_{max} can be attributed to the un-thermal stable nitrogen-containing group in the PBTP. At high temperature, gas such as HNCO and NH_3 which play the gas phase interrupted flame role are released between 250 °C and 500 °C. Besides, what's worth mentioning is that the residual char obtained in EP/GFR is remarkably higher than EP and EP/GO, increased by 10.4% with only 1 wt% addition. The rich char yield formed during decomposition is due to the condensed phase flame retardant mechanism of both

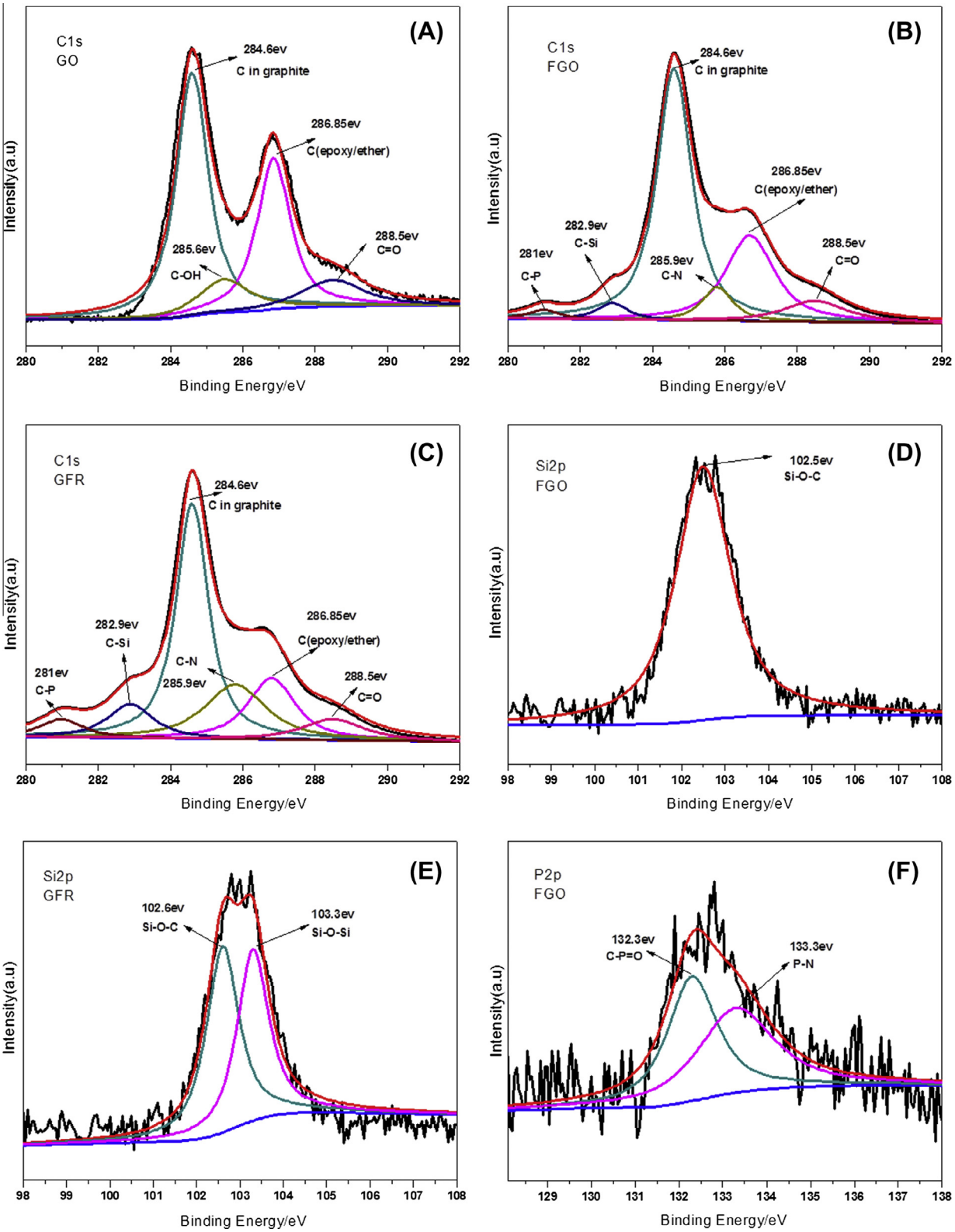

Fig. 3. XPS spectra of GO, FGO and GFR: (A) GO-C1s; (B) FGO-C1s; (C) GFR-C1s; (D) FGO-Si2p; (E) GFR-Si2p and (F) FGO-P2p.

phosphorus and silicon elements in GFR which can block the fuel and oxygen between composites and the environment as well as hinder the heat transfer. All the above indicates that the GFR is more an effective flame retardant additive than a thermal stability additive.

3.5. Flame retardance and combustion performance of EP/GFR composites

The LOI results of EP/GO and EP/GFR composites are showed in Fig. 9. The LOI of pure EP is 20 and increases as the content of either

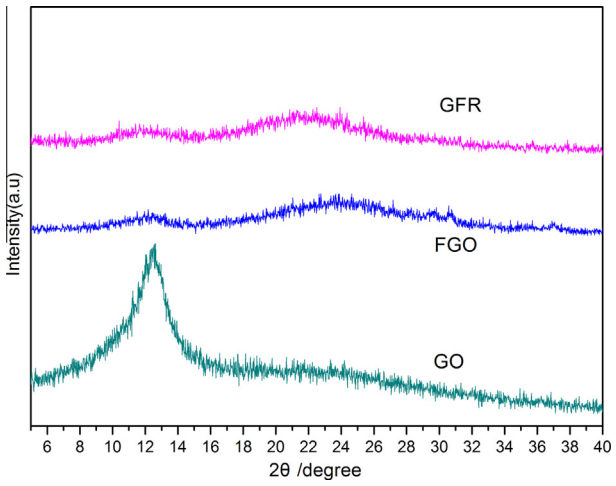

Fig. 4. XRD spectra of GO, FGO and GFR.

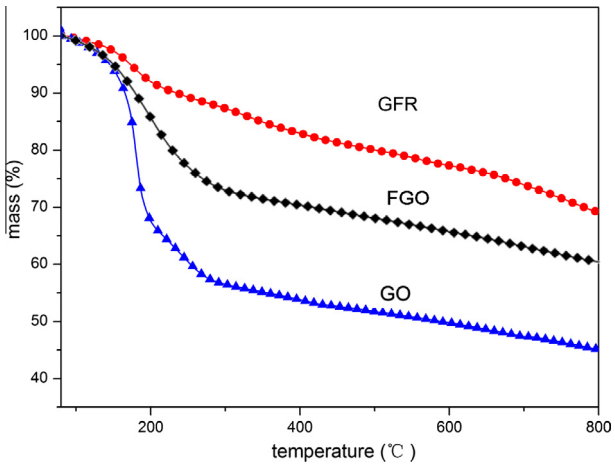

Fig. 6. TGA curves of GO and GFR at heating rate 10 °C/min under N_2.

GO or GFR increases. Compared to GO's lower contribution to EP's fire behavior, GFR contributes much more to enhancing EP's flame retardance. 25 of LOI can be reached with only 2wt% addition of GFR, with the same amount of GO, the LOI is only 22.5.

The micro-cone calorimeter test is used to measure the combustion performance of EP and EP composites which was carried out on pyrolysis-combustion flow calorimeter (PCFC). The heat release rates versus time curves for EP, EP/GO and EP/GFR composites are showed in Fig. 10. The data of heat release rate (HRR) and heat release capacity (HR) are listed in Table 2. The content of GO and GFR addition are both only 1 wt%.

The peak HRR of EP composites remarkably reduce whether when adding GFR or GO, but the EP/GFR composites decreased strongly by 44.7%, while the decrease of EP/GO peak HRR is only 18% compared to that of pure EP, besides, the HR value of EP/GFR composites reduces from 230 to 131 J g^{-1} k^{-1}, which indicates that

Table 1
TGA data of GO, GFR, EP and its composites.

Sample	$T_{5\%}$ (°C)	T_{max} (°C)	Residual char 800 °C (%)
GO	143	–	45.2
FGO	157		61
GFR	175	–	70
EP	315	365	2.7
EPGO1	290	358	3.2
EPGFR0.5	310	346	8.3
EPGFR1	303	340	13.1
EPGFR2	299	328	15.2

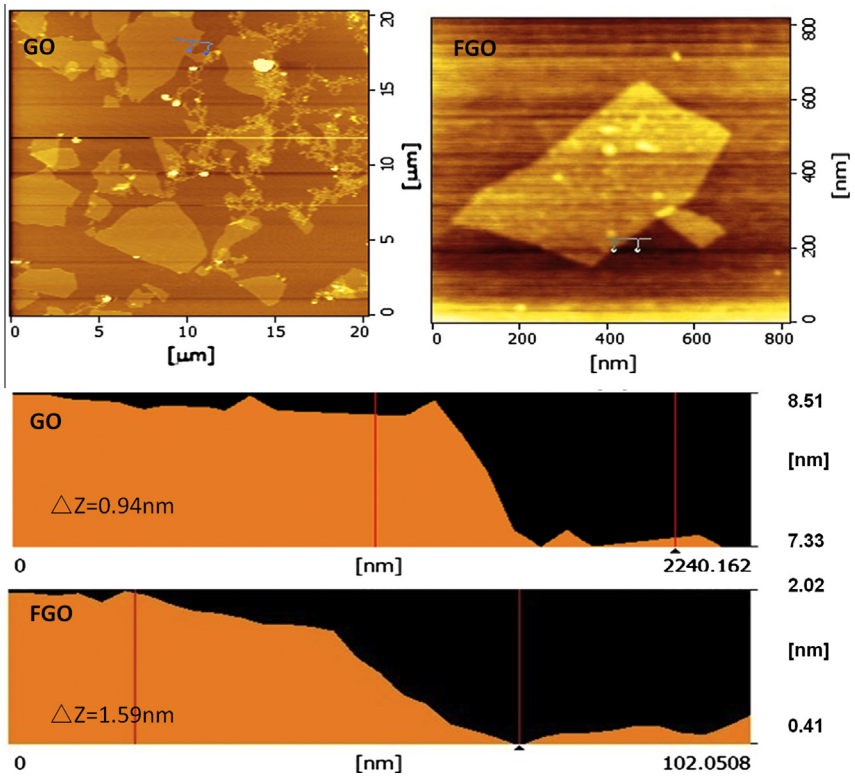

Fig. 5. AFM images and height profiles of GO and FGO sheets.

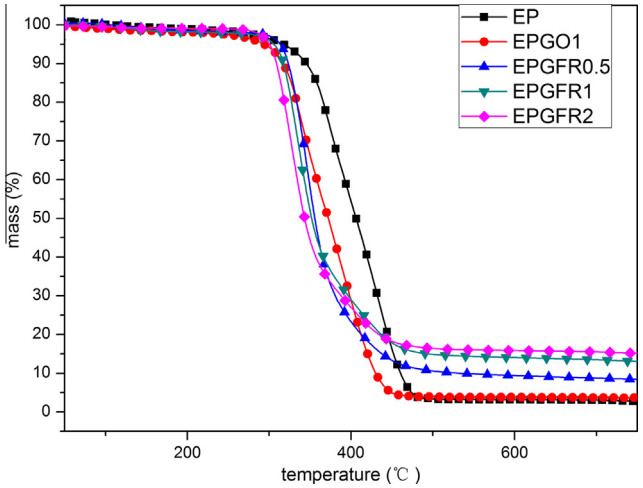

Fig. 7. TGA curves of EP and EP composites at heating rate 10 °C/min under N_2.

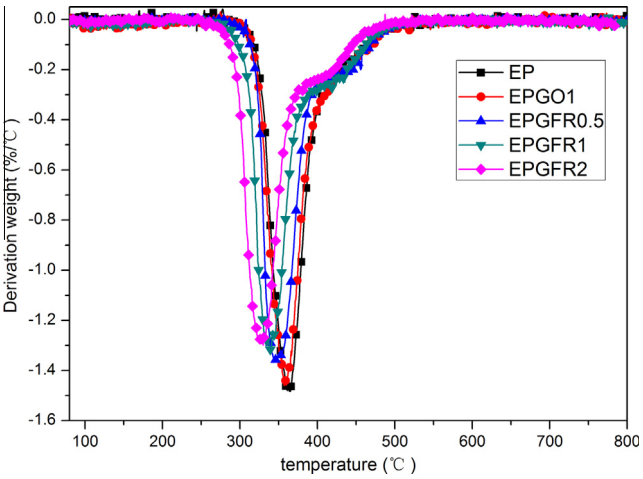

Fig. 8. DTG curves of EP and EP composites at heating rate 10 °C/min under N_2.

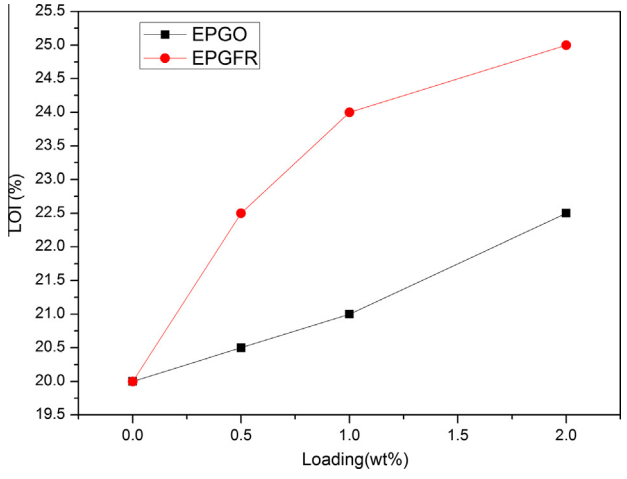

Fig. 9. LOI data of EP composites with different loading of GO and GFR.

GFR is an effective flame retardant additive for EP. In the flame, the silane netted structure around the polyaromatic carbon structures provided by graphene could protect the polymer matrix from decomposing. Besides, the interaction between phosphorus and

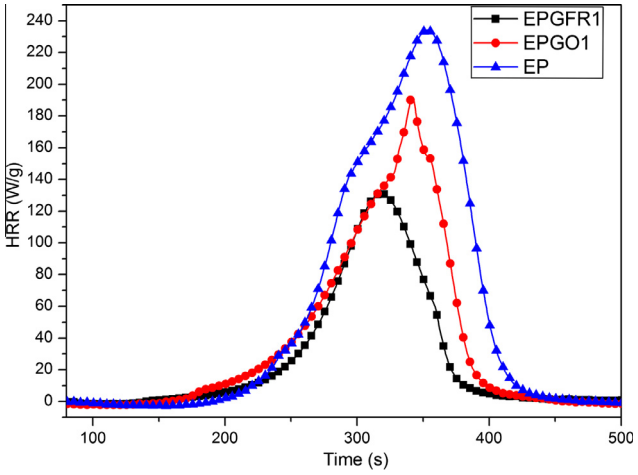

Fig. 10. HRR curves of EP and EP composites in the PCFC test.

Table 2
PCFC data of EP and EP composites.

Sample	Heat release capacity ($J\ g^{-1}\ k^{-1}$)	Peak value of heat release rate (w/g)
EP	230	235.6
EP/GO1	191	193.5
EP/GFR1	131	131.3

silicon can lead to the formation of new linkages such as —P(=O)—O—Si— and act as bridges to connect the three dimensional net of Si—O—Si framework and polyaromatic carbon structures of the graphene [32], which would increase both the quantity and thermal stability of the char. The synergism effect of nitrogen, phosphorus and silicon elements combine the gas phase and the condensed phase flame retardant mechanism, strongly enhance the combustion behavior of EP in the real fire.

3.6. Char morphology analysis

SEM is used to evaluate the morphology of residual char after combustion. Fig. 11 shows the outer and inner char morphology of GO/EP (A and C) and GFR/EP (B and D) after LOI test. Homogeneous outer char without any cracking and continuous neat and dense structure is observed in GFR/EP composites, the rough morphology of inner char is formed by impact of internal degraded gas. In GO/EP composites, the char is extremely messy and crushed. Big air holes appear in outer char layer. It indicates that the GFR can promote the formation of dense char layer and enhancing char stability, which is in accord with results showed in TGA analysis.

3.7. DMA mechanical properties of EP/GFR composites

Dynamic mechanical analysis (DMA) was used to evaluate the mechanical properties of EP/GFR composites. Fig. 12 shows the storage modulus curves and loss angle tangent of EP/GFR composites. The storage modulus of the EP composites increase simultaneously and then decline with the increase of GFR. The storage modulus of pure EP at 25 °C is 1266 MPa. When adding 2 wt% of GFR, the storage modulus of EP composites was increased by 57% and reached 1982 MPa. However, continuous addition of GFR failed to present a continuous increase of storage modulus, it is 1410 MPa when the GFR amount reached 3 wt% of the composites, lower than

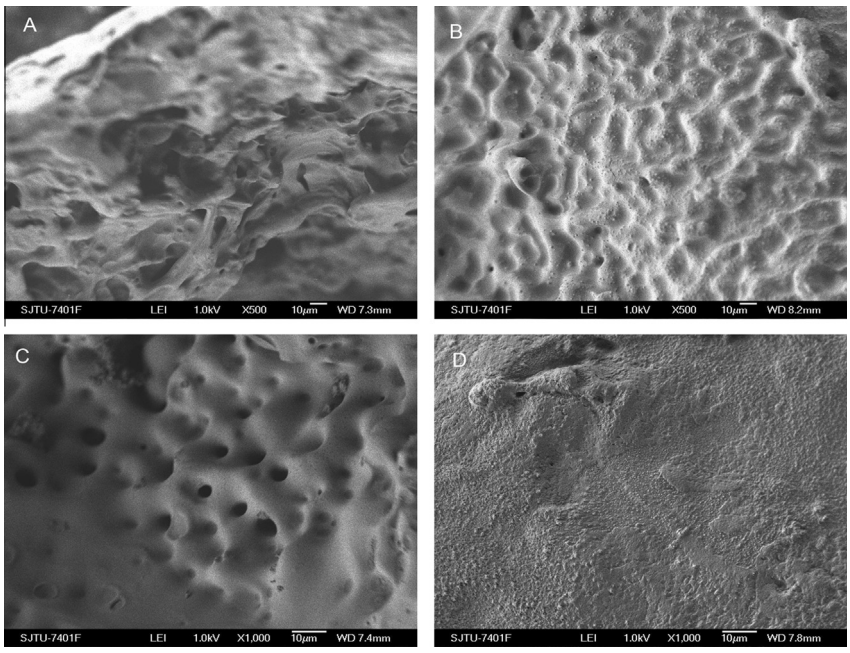

Fig. 11. SEM images of char residual after LOI tests: (A) inner char residual of GO/EP; (B) inner char residual of GFR/EP; (C) outer char residual of GO/EP and (D) outer char residual of GFR/EP.

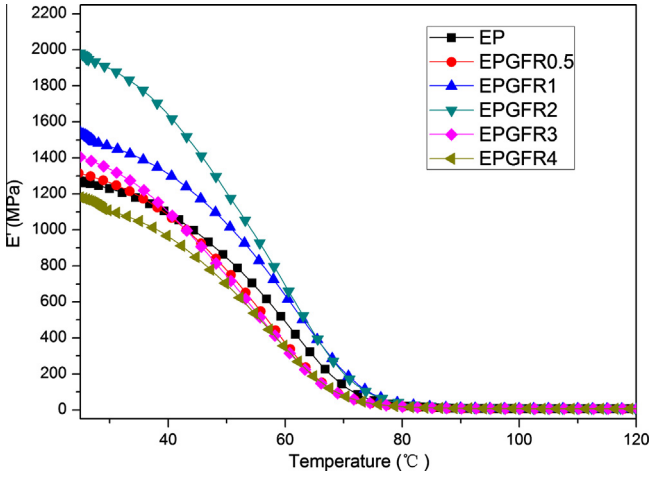

Fig. 12. Storage modulus curves of EP and GFR/EP composites in the DMA test.

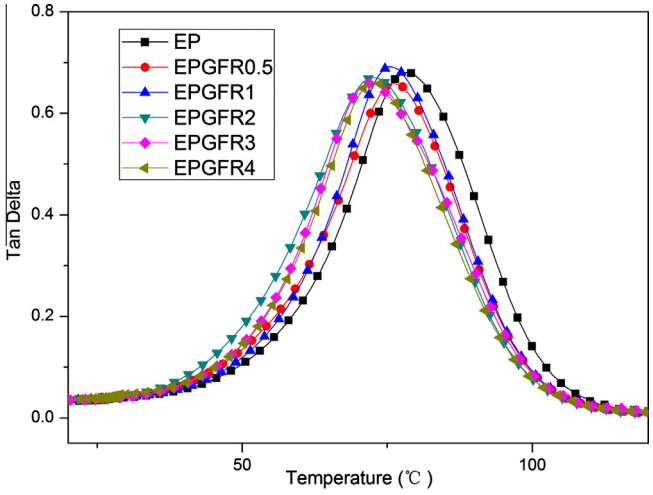

Fig. 13. Tan delta curves of EP and EP/GFR composites in the DMA test.

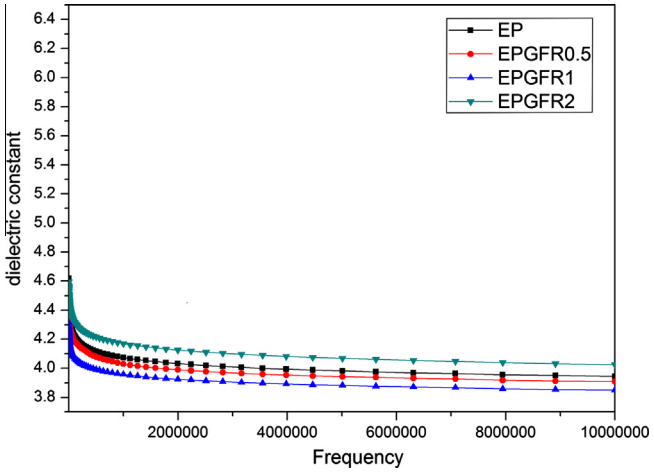

Fig. 14. Dielectric constant of EP and EP/GFR composites.

Table 3
Conductivity of EP and EP/GFR composites.

Sample	EP	EP/GFR0.5	EP/GFR1	EP/GFR2
Conductivity (S/m)	1.04E−08	1.42E−08	1.58E−08	2.89E−08

when only 1% GFR were added. When it contained 4 wt% GFR, the storage modulus decreased to 1178 MPa, even lower than that of the pure EP. This is ascribed to that excessive amount of GFR affected the cross-linked structure between the EP molecular chains and the curing agent. The reduced cross-linking density of EP leads to decreased mechanical properties. This "cross-linking density" effect has been discussed in the early report [3]. The glass transition temperature (Tg) corresponds to the maximum of loss factor (Fig. 13). For pure EP, the Tg occurs at 78.7 °C, with the addition of GFR, it shifts to lower temperature, which indicates that a plasticizer role played by GFR increased the flexibility of chain segments of EP matrix.

3.8. Electrical properties of EP/GFR composites

Fig. 14 and Table 3 are dielectric constants of EP/GFR composites under different frequencies and their conductivity respectively. The conductivity and dielectric constants of testing samples with different GFR addition amount are nearly the same, the dielectric constants are even slightly reduced with low GFR loading (below 1%). This is mainly because that although the PBTP removed the oxygen groups of GO sheets, the π-electron conjugation system was not recovered completely. The links between each GO sheets are insulating PBTP, failing to form the impacted structure, which limit the transfer of free electrons. In this way, the applications of epoxy resin in diverse electrical apparatus area are remained.

4. Conclusion

In this paper, a novel graphene-based hybrid flame retardant GFR containing phosphorus, nitrogen and silicon was synthesized whose structure was verified by FT-IR, XPS, XRD and TGA. The EP/GFR epoxy composites were prepared and their thermal stability and flammability properties were investigated. The residual char obtained in EP/GFR is remarkably higher than EP and EP/GO, increased by 10.4% with only 1 wt% addition. The TG results demonstrated that the char residual can be considerably promoted due to rich flame retardant elements in GFR. A significant reduction of HR and HRR present in PCFC test, reduced strongly by 43% and 44.7% respectively with loading of only 1 wt% GFR, which indicates a good flame retardant effect of GFR in the EP composites. Besides, the GFR can also improved the storage modulus and increased the flexibility of chain segments of EP matrix, meanwhile, the electrical properties such as electric insulativity and dielectric properties were retained.

Acknowledgements

This work is financially supported by the National Natural Science Foundation of China for the Projects (Grant numbers: 51173106 and 51133003). The Instrumental Analysis Center of Shanghai Jiao Tong University is acknowledged for testing support.

References

[1] Miller SG, Bauer JL, Maryanski MJ, Heimann PJ, Barlow JP, Gosau J-M, et al. Characterization of epoxy functionalized graphite nanoparticles and the physical properties of epoxy matrix nanocomposites. Compos Sci Technol 2010;70(7):1120–5.
[2] Guo Y, Bao C, Song L, Yuan B, Hu Y. In situ polymerization of graphene, graphite oxide, and functionalized graphite oxide into epoxy resin and comparison study of on-the-flame behavior. Ind Eng Chem Res 2011;50(13):7772–83.
[3] Bao C, Guo Y, Song L, Kan Y, Qian X, Hu Y. In situ preparation of functionalized graphene oxide/epoxy nanocomposites with effective reinforcements. J Mater Chem 2011;21(35):13290.
[4] Chiang C-L, Hsu S-W. Novel epoxy/expandable graphite halogen-free flame retardant composites–preparation, characterization, and properties. J Polym Res 2009;17(3):315–23.
[5] Kuan C-F, Yen W-H, Chen C-H, Yuen S-M, Kuan H-C, Chiang C-L. Synthesis, characterization, flame retardance and thermal properties of halogen-free expandable graphite/PMMA composites prepared from sol–gel method. Polym Degrad Stab 2008;93(7):1357–63.
[6] Schartel B, Knoll U, Hartwig A, Pütz D. Phosphonium-modified layered silicate epoxy resins nanocomposites and their combinations with ATH and organophosphorus fire retardants. Polym Adv Technol 2006;17(4):281–93.
[7] Sun J, Wang X, Wu D. Novel spirocyclic phosphazene-based epoxy resin for halogen-free fire resistance: synthesis, curing behaviors, and flammability characteristics. ACS Appl Mater Interfaces 2012;4(8):4047–61.
[8] Zhang K, Shen M-M, Wu K, Liu H-F, Zhang Y. Comparative study on flame retardancy and thermal degradation of phosphorus- and silicon-containing epoxy resin composites. J Polym Res 2011;18(6):2061–70.
[9] Tarrío-Saavedra J, López-Beceiro J, Naya SArtiaga R. Effect of silica content on thermal stability of fumed silica/epoxy composites. Polym Degrad Stab 2008;93(12):2133–7.
[10] Chiang C, Chang R. Synthesis, characterization and properties of novel self-extinguishing organic–inorganic nanocomposites containing nitrogen, silicon and phosphorus via sol–gel method. Compos Sci Technol 2008;68(14):2849–57.
[11] Chiang C-L, Chang R-C, Chiu Y-C. Thermal stability and degradation kinetics of novel organic/inorganic epoxy hybrid containing nitrogen/silicon/phosphorus by sol–gel method. Thermochim Acta 2007;453(2):97–104.
[12] Potts JR, Dreyer DR, Bielawski CW, Ruoff RS. Graphene-based polymer nanocomposites. Polymer 2011;52(1):5–25.
[13] Teng C-C, Ma C-CM, Lu C-H, Yang S-Y, Lee S-H, Hsiao M-C, et al. Thermal conductivity and structure of non-covalent functionalized graphene/epoxy composites. Carbon 2011;49(15):5107–16.
[14] Ramanathan T, Abdala AA, Stankovich S, Dikin DA, Herrera-Alonso M, Piner RD, et al. Functionalized graphene sheets for polymer nanocomposites. Nat Nanotechnol 2008;3(6):327–31.
[15] Wang Y, Shi Z, Fang J, Xu H, Yin J. Graphene oxide/polybenzimidazole composites fabricated by a solvent-exchange method. Carbon 2011;49(4):1199–207.
[16] Hou S, Su S, Kasner ML, Shah P, Patel K, Madarang CJ. Formation of highly stable dispersions of silane-functionalized reduced graphene oxide. Chem Phys Lett 2010;501(1–3):68–74.
[17] Kim H, Abdala AA, Macosko CW. Graphene/polymer nanocomposites. Macromolecules 2010;43(16):6515–30.
[18] Sun Y, Li C, Xu Y, Bai H, Yao Z, Shi G. Chemically converted graphene as substrate for immobilizing and enhancing the activity of a polymeric catalyst. Chem Commun 2010;46(26):4740.
[19] Wang X, Song L, Yang H, Xing W, Kandola B, Hu Y. Simultaneous reduction and surface functionalization of graphene oxide with POSS for reducing fire hazards in epoxy composites. J Mater Chem 2012;22(41):22037.
[20] Matsuo Y, Nishino Y, Fukutsuka T, Sugie Y. Introduction of amino groups into the interlayer space of graphite oxide using 3-aminopropylethoxysilanes. Carbon 2007;45(7):1384–90.
[21] Liao S-H, Liu P-L, Hsiao M-C, Teng C-C, Wang C-A, Ger M-D, Chiang C-L. One-step reduction and functionalization of graphene oxide with phosphorus-based compound to produce flame-retardant epoxy nanocomposite. Ind Eng Chem Res 2012;51(12):4573–81.
[22] Yang H, Li F, Shan C, Han D, Zhang Q, Niu L, et al. Covalent functionalization of chemically converted graphene sheets via silane and its reinforcement. J Mater Chem 2009;19(26):4632.
[23] Ciesielski M, Schäfer A, Döring M. Novel efficient DOPO-based flame-retardants for PWB relevant epoxy resins with high glass transition temperatures. Polym Adv Technol 2008;19(6):507–15.
[24] Qian Y, Wei P, Jiang P, Liu J. Preparation of halogen-free flame retardant hybrid paraffin composites as thermal energy storage materials by in situ sol–gel process. Sol Energy Mater Sol Cells 2012;107:13–9.
[25] Qian Y, Wei P, Jiang P, Zhao X, Yu H. Synthesis of a novel hybrid synergistic flame retardant and its application in PP/IFR. Polym Degrad Stab 2011;96(6):1134–40.
[26] Feldtner N, Brockner W, Scharff P, Dadras MM. Novel carbon materials obtained by reactions of C60 fullerene with phosphorus at high temperature. J Non-Cryst Solids 2004;333(3):301–6.
[27] Rosas JM, Ruiz-Rosas R, Rodríguez-Mirasol J, Cordero T. Kinetic study of the oxidation resistance of phosphorus-containing activated carbons. Carbon 2012;50(4):1523–37.
[28] Rupper P, Gaan S, Salimova V, Heuberger M. Characterization of chars obtained from cellulose treated with phosphoramidate flame retardants. J Anal Appl Pyrol 2010;87(1):93–8.
[29] Zhang D, Liu X, Wang X. Green synthesis of graphene oxide sheets decorated by silver nanoprisms and their anti-bacterial properties. J Inorg Biochem 2011;105(9):1181–6.
[30] Liu S, Tian J, Wang L, Sun X. Microwave-assisted rapid synthesis of Ag nanoparticles/graphene nanosheet composites and their application for hydrogen peroxide detection. J Nanopart Res 2011;13(10):4539–48.
[31] Song C, Wu D, Zhang F, Liu P, Lu Q, Feng X. Gemini surfactant assisted synthesis of two-dimensional metal nanoparticles/graphene composites. Chem Commun 2012;48(15):2119.
[32] Zhang W, Li X, Fan H, Yang R. Study on mechanism of phosphorus–silicon synergistic flame retardancy on epoxy resins. Polym Degrad Stab 2012;97(11):2241–8.